PERGAMON

Corrosion Science 43 (2001) 1557–1572

CORROSION SCIENCE

www.elsevier.com/locate/corsci

Raman spectroscopic analysis of the speciation of dilute chromate solutions

Jeremy D. Ramsey [a], Lin Xia [a], Martin W. Kendig [b], Richard L. McCreery [a,*]

[a] *Department of Chemistry, The Ohio State University, 100 W. 18th Avenue, Columbus, OH 43210, USA*
[b] *Rockwell Science Center, 1049 Camino Dos Rios, Thousand Oaks, CA 91360, USA*

Received 19 April 2000; accepted 14 August 2000

Abstract

The relative concentrations of various Cr^{VI} species are important to several mechanisms for corrosion inhibition by chromate conversion coatings and chromate containing primers. The pH dependent conversion of CrO_4^{-2} to $Cr_2O_7^{-2}$ is well known, but the existence and importance of bichromate, $HCrO_4^-$, is more controversial. Past reports have described the pH and concentration dependence of the $CrO_4^{-2}/HCrO_4^-/Cr_2O_7^{-2}$ distribution, while recent reports have concluded that $HCrO_4^-$ does not exist in aqueous media. The current work shows that $HCrO_4^-$ does indeed exist at a pH below 6 and at low total Cr^{VI} concentration. The Raman signature of the Cr–O–Cr bond in dichromate decreases relative to the Cr–O symmetric stretch as $[Cr^{VI}]$ decreases. The results are quantitatively consistent with previous reports on the $CrO_4^{-2}/HCrO_4^-/Cr_2O_7^{-2}$ equilibrium, and establish that $HCrO_4^-$ is the dominant Cr^{VI} species for low $[Cr^{VI}]$. In the low concentration and slightly acidic conditions likely to be present during corrosion inhibition by Cr^{VI} in the field, $HCrO_4^-$ is the most prevalent form of Cr^{VI} in water.

1. Introduction

Cr^{VI} oxides have been shown to be very effective corrosion inhibitors for aluminum alloys as well as other metals. These oxides are normally deposited onto the metal in the form of a film or chromium conversion coating (CCC), but chromates

* Corresponding author. Fax: +1-614-688-5402.
E-mail address: mccreery.2@osu.ed (R.L. McCreery).

0010-938X/01/$ - see front matter
PII: S0010-938X(00)00145-1

are also effective solution corrosion inhibitors. Xia and McCreery have shown that the conversion coatings consist of a Cr^{III} hydroxide polymer backbone with adsorbed Cr^{VI} oxides [1]. Of special interest is the "self-healing" property inherent to CCC films. An intact CCC has been observed to protect an uncoated sample from corrosion through the release of soluble Cr^{VI} oxides into solution [2]. Under conditions of low Cr^{VI} concentration ($<10^{-3}$ M) and moderate acidity (pH 5–6), released Cr^{VI} not only increased the corrosion resistance of the sample, but was also deposited on the surface of the uncoated alloy as an Al^{III}/Cr^{VI} mixed oxide [2,3].

It has been observed that Cr^{VI} adsorption to passive oxide films may be particularly important to the corrosion inhibition mechanism. McCafferty proposed competitive adsorption as the corrosion inhibition mechanism for Cr^{VI} on iron surfaces [4]. The critical ratio of adsorbed chloride to adsorbed Cr^{VI} species allowed for corrosion protection was calculated. Piezoelectrokinetic (PEK) measurements of Cr^{VI} adsorption onto aluminum oxide surfaces indicate that Cr^{VI} adsorption significantly reduces the zeta potential of the alumina substrate [5]. This data supports the theory that chromate adsorption may discourage chloride adsorption through a change in the surface charge. There is also an implication that the speciation of the solution phase Cr^{VI} is important to the inhibition mechanism.

The concentrations of Cr^{VI} observed in corrosion systems can vary greatly. In the coating process (Alodine 1200S), the concentration of Cr^{VI} is relatively high (0.05 M) and the bath pH is between 1 and 2. Conversely, under field or self-healing conditions, Cr^{VI} is quite low. Release of Cr^{VI} from a damaged conversion coating has been shown to be only 0.2 mM at near neutral pH [6]. The stark contrast in environments necessitates the understanding of the speciation in aqueous systems. Differing speciation may have a dramatic effect on Cr^{VI} adsorption characteristics on metal oxide surfaces as well as on the stability constants of corrosion products.

The speciation of Cr^{VI} in aqueous solution has been extensively studied using techniques such as spectrophotometry [7–12], electrochemistry [11,13–15], freezing point depression [16], and nuclear magnetic resonance (NMR) [17,18]. Although these techniques do not provide direct molecular evidence of the structure of Cr^{VI} in solution, they do substantiate the accepted equilibria that are outlined by Eqs. (1)–(3).

$$H_2CrO_4 \rightleftharpoons H^+ + HCrO_4^-, \qquad K_1 = \frac{[H^+][HCrO_4^-]}{[H_2CrO_4]} \tag{1}$$

$$HCrO_4^- \rightleftharpoons H^+ + CrO_4^{-2}, \qquad K_2 = \frac{[H^+][CrO_4^{-2}]}{[HCrO_4^-]} \tag{2}$$

$$2HCrO_4^- \rightleftharpoons Cr_2O_7^{-2} + H_2O, \qquad K_d = \frac{[Cr_2O_7^{-2}]}{[HCrO_4^-]^2} \tag{3}$$

Recently, the existence of the bichromate ion ($HCrO_4^-$) has been questioned [19–21]. Under conditions where $HCrO_4^-$ was predicted to be the predominant solution species, no change in the Raman spectrum from that of $Cr_2O_7^{-2}$ was observed

[19,20,22]. Using spectrophotometry, Poulopoulou et al. proposed that $HCrO_4^-$ is a strong acid and present at concentrations below the detection limits for both Raman spectroscopy and UV–VIS spectrophotometry [21].

The toxicity of Cr^{VI} [23–25] is an additional factor that motivates the clarification of this controversy. Cr^{VI} has been shown to increase the occurrence of genetic mutations [23] and skin ulcerations [24]. More importantly, significant evidence indicates that hexavalent chromium is a carcinogen [25]. Environmental exposure to Cr^{VI} is usually at quite low concentration, where the speciation of CrO_4^{-2}, $HCrO_4^-$, and $Cr_2O_7^{-2}$ is least well understood. Understanding both the toxicity and corrosion protection of dilute Cr^{VI} solutions is an important step toward developing environmentally benign replacements.

Raman spectroscopy is well suited to the study of Cr^{VI} compounds, due to its molecular specificity and compatibility with water. Applications that include the fields of catalysis [26] and corrosion [1–3,6] illustrate the utility of Raman for this purpose. The advent of holographic filters, FT-Raman, and charge coupled device (CCD) technology has greatly improved the sensitivity of Raman spectroscopy over the past 10–15 years. The current report involves the application of modern, high sensitivity Raman spectroscopy to the question of Cr^{VI} speciation at low concentrations.

2. Experimental

2.1. Reagents

All chemicals were of reagent grade and used as received. All solutions were prepared using "Nanopure" water (Barnstead) with a minimum resistivity of 18 MΩ. Cr^{VI} solutions were prepared by dissolving potassium dichromate or Cr^{VI} oxide in HCl or NaOH solutions of known pH. If necessary, the solution pH was adjusted to the desired level using concentrated solutions of HCl and NaOH. Potassium nitrate was also included in the solutions as an internal standard for Raman shift frequency and intensity as well as an ionic strength adjuster.

2.2. Spectroscopy

Most of the Raman spectra in this study were recorded using a Bruker FRA106/S Fourier transform (FT) Raman module coupled to a Bruker 66S FT infrared absorption spectrometer. A Ge based detector cooled to $< -110°C$ with liquid nitrogen was used to record the Raman interferogram. A 1064 nm Nd-YAG laser was used as the excitation source and the resulting Raman and Rayleigh scattered light was collected and filtered using a proprietary Bruker rejection filter. To record the spectra in this study, either 512 or 1024 scans of the interferometer with 380 mW of laser power at the sample were used to achieve an adequate signal to noise ratio. A background of water in a cuvette was subtracted from each of the Raman spectra. The measurements were repeated for several concentrations and pH values using a

Chromex IS250 dispersive spectrometer capable of operating at both 488 and 514.5 nm excitation. All Raman spectra were analyzed using GRAMS/32 spectroscopic analysis software (Galatic, Salem, New Hampshire, Version 4.02)

2.3. Equilibrium calculations

The equilibrium speciation calculation has been described by others [27–29], however it will be reviewed briefly here. The equilibria of Cr^{VI} species in aqueous solution may be described in terms of the equilibrium constants expressed in Eqs. (1)–(3). After expressing $[H_2CrO_4]$, $[Cr_2O_7^{-2}]$, and $[CrO_4^{-2}]$, in terms of $[HCrO_4^-]$, the mass balance expression for Cr^{VI} may be employed to calculate equilibrium concentrations of all Cr^{VI} species as functions of pH and total Cr^{VI} concentration, $[Cr^{VI}]_{total}$. Although several values for K_1, K_2, and K_d have been reported for a range of ionic strengths, values for low ionic strength as well as those appropriate to the high ionic strengths used here are listed in Table 1.

3. Results

As Eqs. (1)–(3) indicate, Cr^{VI} equilibria are dependent on pH, with $Cr_2O_7^{-2}$ and $HCrO_4^-$ existing primarily in acidic media and CrO_4^{-2} being the lone solution species above pH 7. Fig. 1 shows the distribution of Cr^{VI} species calculated from Eqs. (1)–(3) for $[Cr^{VI}]_{total} = 0.05$ M. At high Cr^{VI} concentrations, dimer formation is favorable and $Cr_2O_7^{-2}$ is predominant. With $[Cr^{VI}]_{total} = 1$ M, for example, 94% of the Cr^{VI} is present as $Cr_2O_7^{-2}$ at pH 3, with the remainder as $HCrO_4^-$. For pH 3 and $[Cr^{VI}]_{total} = 10^{-4}$ M, only 1% of the Cr^{VI} is in the form of $Cr_2O_7^{-2}$. These predictions assume that Eqs. (1)–(3) are correct and that $HCrO_4^-$ exists.

Raman spectroscopy was used to probe the structure of the Cr^{VI} species due to the structural information inherent in the technique. Fig. 2 shows the spectra of three different crystalline Cr^{VI} compounds. Although many of the bands are split for the crystalline materials, it is obvious that Cr^{VI} oxides possess strong characteristic Raman bands in the range of 850–1000 cm^{-1}. These bands have previously been assigned to Cr–O stretching modes [30–33]. More importantly, the dimeric

Table 1
Literature values for Cr^{VI} equilibrium constants

Constant	Value	Ionic strength (M)	Reference
K_1	1.21	1	[7]
	0.18	0.16	[13]
K_2	1.62×10^{-6}	1.5	[15]
	3.2×10^{-7}	0	[7]
K_d	138	1.5	[15]
	35.5	0.33–0.63	[13]

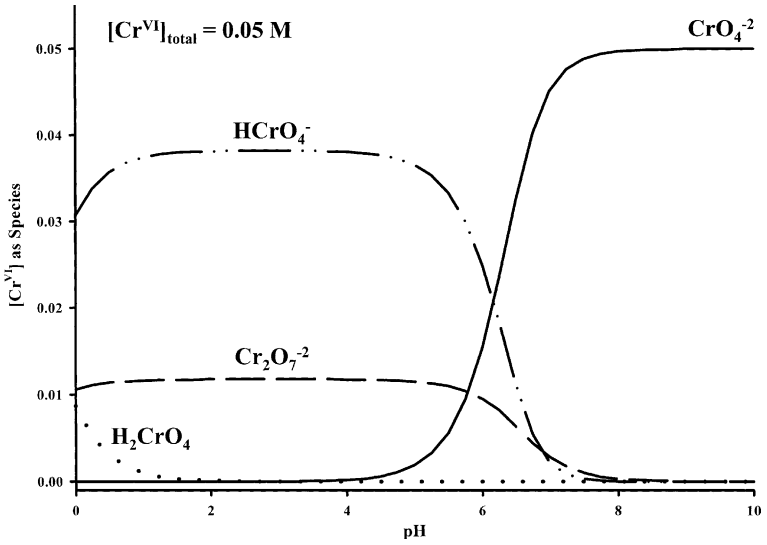

Fig. 1. The distribution of Cr^{VI} species in aqueous solution as a function of pH. The lines represent H_2CrO_4 (···), $Cr_2O_7^{-2}$ (– – –), $HCrO_4^-$ (–·–), and CrO_4^{-2} (—). A Cr^{VI} concentration of 0.05 M and the equilibrium constants from Table 1 were used for the calculation.

($K_2Cr_2O_7$) and polymeric (CrO_3) Cr^{VI} oxides possess Cr–O–Cr bridging vibrations. The bands in the range between 200 and 240 cm^{-1} have been assigned to the bending mode of the bridge [30,31]. Monomeric species (K_2CrO_4) do not possess these modes. Raman spectra of aqueous solutions of Cr^{VI} are qualitatively similar to the crystalline with the exception of the lattice splitting modes observed in the solids. Table 2 contains the literature assignment of the vibrations of aqueous CrO_4^{-2}, $HCrO_4^-$, and $Cr_2O_7^{-2}$. Note that CrO_3 is not a stable solution species and upon dissolution in water it equilibrates to the stable solution species (CrO_4^{-2}, $Cr_2O_7^{-2}$, $HCrO_4^-$).

The characteristic Raman features in the range of 850–1000 cm^{-1} can be used as a quantitative marker for total Cr^{VI} concentration. A calibration curve was constructed using solutions of various Cr^{VI} concentration that had been adjusted to a pH of 2. Fig. 3 shows that the area of the ~900 cm^{-1} band scales linearly with an increase in total Cr^{VI} concentration. This observation appears to be contrary to Eqs. (1)–(3), which indicate that the solution speciation of Cr^{VI} would vary over this range. However, even with a changing solution composition, the ~900 cm^{-1} band serves as a marker for the total concentration of Cr^{VI}. Apparently, the cross section for $Cr_2O_7^{-2}$ stretching is approximately twice that of $HCrO_4^-$, resulting in linear behavior of Cr^{VI}–O intensity vs. [Cr^{VI}]. A more detailed discussion of this observation requires consideration of the relationship between Raman intensity and concentration.

The signal observed in a Raman experiment can be described using Eq. (4).

$$S_A = P_D \beta_A D_A \Omega A_D T(\lambda) Q(\lambda) K t \tag{4}$$

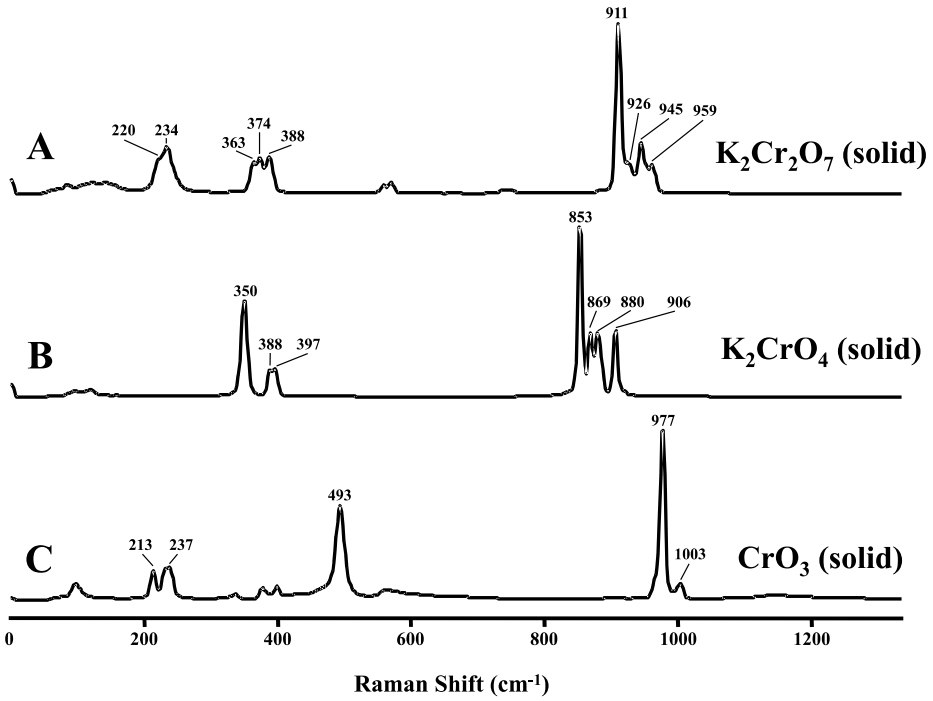

Fig. 2. Raman spectra of reagent grade Cr^{VI} compounds obtained using the Bruker FRA106/S FT Raman Module (resolution = 4.0). (A) $K_2Cr_2O_7$ (B) K_2CrO_4 (C) CrO_3.

Derivation of this expression has been presented previously [34] and only a brief explanation of the equation will be provided here. The sample dependent parameters consist of P_D, the laser power density in photons $s^{-1}\,cm^{-2}$; β_A, the scattering cross-section of a specific vibration of the analyte in cm^2 molecules^{-1} sr^{-1}; and D_A, the number density of the analyte in molecules cm^{-3}. The spectrometer and detector parameters consist of Ω, the collection angle of the spectrometer in sr; A_D, the area of the sample monitored by the spectrometer in cm^2; $T(\lambda)$, the transmission efficiency of the optics and spectrometer; $Q(\lambda)$, the quantum efficiency of the detector in electrons photon^{-1}; K, a geometric factor relating the scattering volume to the scattering area; and t, the measurement time in seconds.

The experimental conditions are identical for each of the solutions analyzed in Fig. 3, so a simplified version of Eq. (4) can be written

$$S_N = \frac{S_A}{P_D \Omega A_D T(\lambda) Q(\lambda) K t} = \beta_A D_A \tag{5}$$

where S_N is the analyte signal that has been normalized by the parameters which remain unchanged throughout the Raman experiment. In the case of Cr^{VI}, two

Table 2
Raman shifts for Cr^{VI} modes in solution

Species	Raman shift (cm^{-1})	Vibrational assignment	Reference
$Cr_2O_7^{-2}$	220	δ (Cr–O–Cr)	[30,31]
	365	δ (CrO_3)	
	558	ν_s (Cr–O–Cr)	
	772	ν_{as} (Cr–O–Cr)	
	904	ν_s (CrO_3)	
	946	ν_{as} (CrO_3)	
CrO_4^{-2}	348	δ_d (E)	[32,33]
	368	δ_d (F_2)	
	847	ν_s (A_1)	
	884	ν_d (F_2)	
$HCrO_4^-$	898	ν_s (CrO_3)	[3]

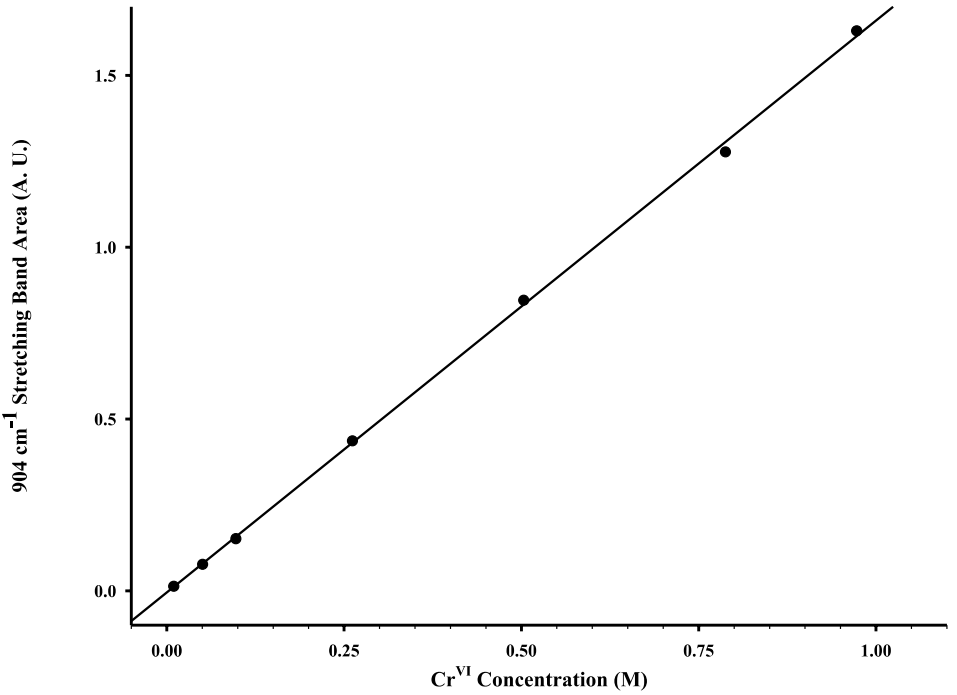

Fig. 3. Plot of ~900 cm^{-1} band area versus solution concentration of Cr^{VI}. The solid line is the result of a linear regression analysis.

scatterers contribute to the signal at ~900 cm^{-1}. This agrees with the recent work of Heyns et al. who concluded that this Raman band is a correlation of dichromate and bichromate signals [22]. Accordingly, a signal expression can be written for the Cr^{VI} species.

$$S_N = \beta_{HCrO_4} D_{HCrO_4} + \beta^{900}_{Cr_2O_7} D_{Cr_2O_7} \quad (6)$$

At low [Cr^{VI}] and moderately acidic pH, the predominant solution species is bichromate and at high [Cr^{VI}], dichromate is the dominant species. If we assume that the concentration of the minority species is zero under these conditions, Eq. (6) simplifies to the following expressions.

$$S_N(\text{low}[Cr^{VI}]) = \beta_{HCrO_4} D_{Cr^{VI}} \quad (7)$$

$$S_N(\text{high}[Cr^{VI}]) = \beta^{900}_{Cr_2O_7} D_{Cr_2O_7} = \tfrac{1}{2}\beta^{900}_{Cr_2O_7} D_{Cr^{VI}} \quad (8)$$

Since the calibration curve is linear over the entire range of Cr^{VI} concentration, and both Eqs. (7) and (8) constitute a segment of the same calibration curve, they must therefore have the same slope. This leads to Eq. (9), relating the cross-section of dichromate to that of bichromate.

$$\tfrac{1}{2}\beta^{900}_{Cr_2O_7} = \beta_{HCrO_4} \quad (9)$$

Upon closer examination of the Raman spectra used to construct Fig. 3, slight changes do occur with Cr^{VI} concentration. The most striking difference is that the actual band frequency changes over this concentration range (Fig. 4A and B). At high Cr^{VI} concentrations (>0.5 M), the symmetric stretching frequency is similar or equal to published values. At lower concentrations, the band shifts toward 898 cm^{-1} and broadens. At pH > 8 and regardless of concentration, no shift is observed as only one species is predicted (Fig. 4C and D). This behavior does not appear to be wavelength dependent since similar results were obtained at 514.5 and 488 nm excitation in addition to the FT Raman data acquired at 1064 nm. Table 3 summarizes the FT Raman results.

The Cr–O–Cr bridging mode was examined as a marker for $Cr_2O_7^{-2}$ concentration. While controlling the pH at 2 and the ionic strength between 1.5 and 2, the total [Cr^{VI}] was varied and the Raman spectra recorded. The resulting Raman spectra are shown in Fig. 5, with the relative intensities adjusted for concentration to provide comparable intensity scales. It is important to note that the 219 cm^{-1} band intensity decreases relative to the 900 cm^{-1} band as the total [Cr^{VI}] is diluted, and is barely detectable at low concentration. Quantitative information about the decline in the band area can be studied after using peak fitting routines from GRAMS to determine peak area. Fig. 6 shows the ratio of the 219 cm^{-1} band area to the ~900 cm^{-1} band area. At low [Cr^{VI}], the ratio varies dramatically indicating that the 219 cm^{-1} band area is decreasing more rapidly than that of the 900 cm^{-1} band. Since the 900 cm^{-1} band area is proportional to $[Cr^{VI}]_{total}$, the 219/900 area ratio provides a quantitative indication of the mole fraction of Cr^{VI} present as $Cr_2O_7^{-2}$.

The expected area of the 219 and 900 cm^{-1} bands can be expressed in terms of the Raman signal Eq. (4). The 219 cm^{-1}/900 cm^{-1} band areas can then be related to the parameters of the Raman signal expression. Eq. (10) assumes that there are only two solution components, bichromate and dichromate, at pH 2.

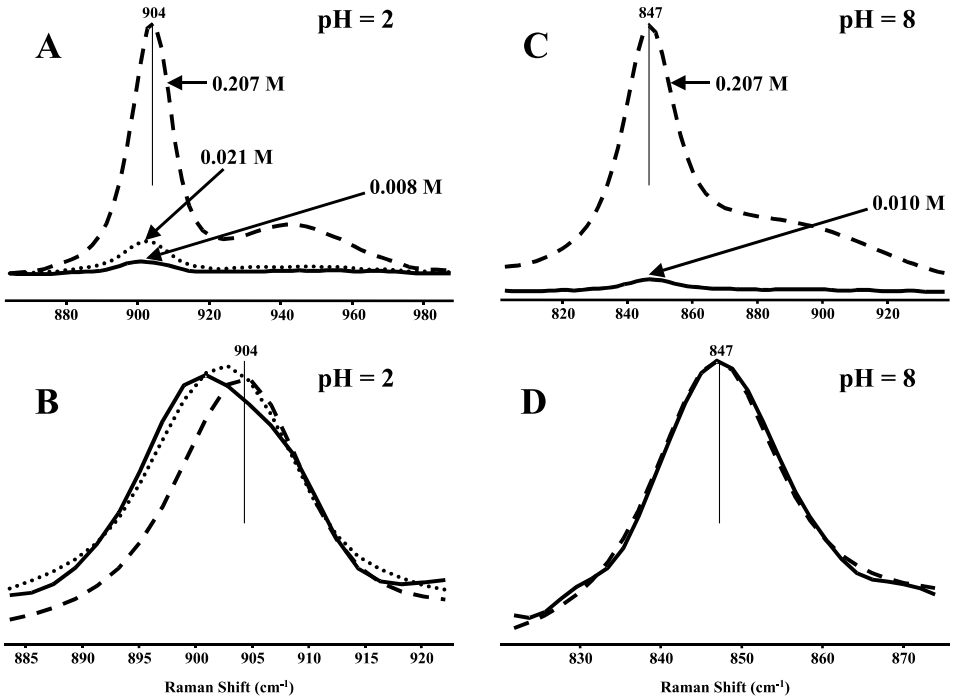

Fig. 4. FT Raman spectra of Cr^{VI} solutions at various concentrations. Plots (A) and (C) are of the Raman signal in the vicinity of the symmetric stretching mode frequency while plots (B) and (D) are magnified to allow visualization of small changes in peak frequency. Cr^{VI} concentrations: Plots (A) and (B), 0.207 M (– – –), 0.021 M (···), 0.008 M (—). Plots (C) and (D), 0.208 M (– – –), 0.010 M (—).

Table 3
Positions and bandwidths of Cr^{VI}–O stretching mode for various pH, concentration, and ionic strength

Ionic strength	$[Cr^{VI}]$ (M)	pH = 2		pH = 8	
		Band position (cm^{-1})	Band width (cm^{-1})	Band position (cm^{-1})	Band width (cm^{-1})
Uncontrolled	0.97	904.77	13.01		
	0.79	904.67	13.17		
	0.50	904.57	13.24		
	0.26	904.24	13.75		
	0.21			846.83	20.45
	0.10	903.81	14.31		
	0.05	903.33	14.90		
	0.01	901.37	15.32	847.24	21.89
1.5–2.0 M	1.00	903.91	11.70		
	0.75	903.81	12.08		
	0.50	903.82	12.23		
	0.25	903.73	12.83		
	0.10	903.38	12.84		
	0.05	902.86	13.58		

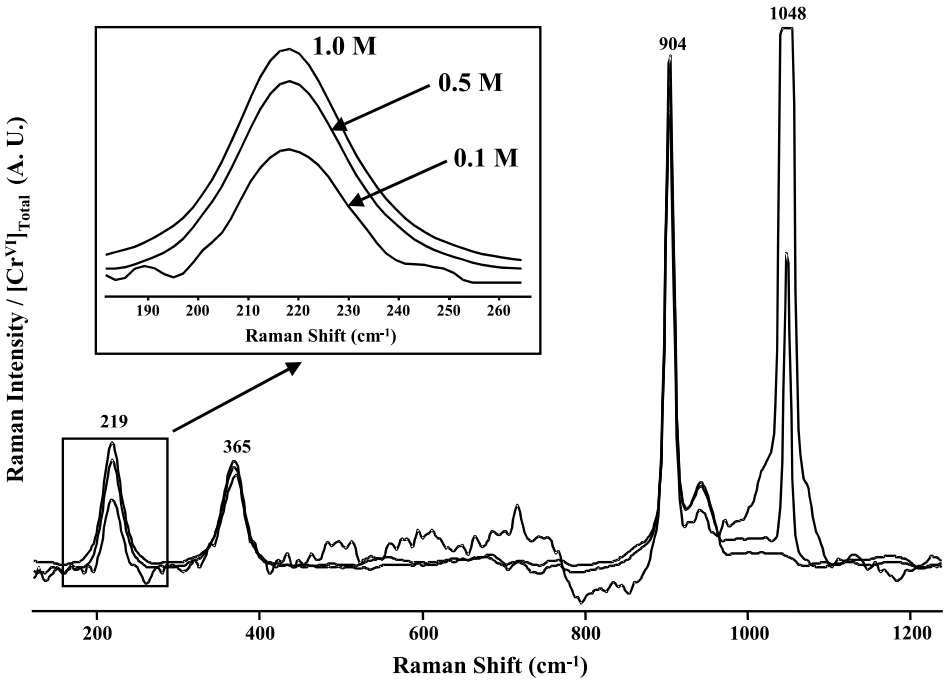

Fig. 5. FT Raman spectra of Cr^{VI} solutions, normalized by total Cr^{VI} concentration. The solutions were adjusted to a pH of 2 and the ionic strength was held between 1.5–2.0 M with potassium nitrate. The inset is an expansion of the spectra near the 219 cm^{-1} bridging mode. Cr^{VI} concentrations: 1.0 M, 0.50 M, and 0.10 M.

$$\frac{\text{area 219 cm}^{-1}}{\text{area 900 cm}^{-1}} = \frac{P_D \Omega A_D T(\lambda) Q(\lambda) K t (\beta^{219}_{Cr_2O_7} D_{Cr_2O_7})}{P_D \Omega A_D T(\lambda) Q(\lambda) K t \left[\beta_{HCrO_4} D_{HCrO_4} + \beta^{900}_{Cr_2O_7} D_{Cr_2O_7}\right]} \tag{10}$$

Because all of the chemical species are exposed to the same experimental conditions, the expression simplifies to Eq. (11).

$$\frac{\text{area 219 cm}^{-1}}{\text{area 900 cm}^{-1}} = \frac{\beta^{219}_{Cr_2O_7} D_{Cr_2O_7}}{\beta_{HCrO_4} D_{HCrO_4} + \beta^{900}_{Cr_2O_7} D_{Cr_2O_7}} \tag{11}$$

The observed ratio is therefore a function of the number densities, which are proportional to the concentration of the individual chemical species, and the Raman scattering cross-section of each of the anions. Eq. (11) can therefore be used to predict the relative concentrations of the Cr^{VI} oxides if the area ratio and the relative cross-sections are known. It also provides qualitative information about the shape of the expected curve under a varying set of conditions.

Substituting the relationship between the cross-section of bichromate and dichromate (Eq. (9)), a correlation between the calculated fraction of Cr^{VI} as dichromate and the area ratio can be established.

$$\frac{\text{area 219 cm}^{-1}}{\text{area 900 cm}^{-1}} = \left(\frac{2\beta^{219}_{Cr_2O_7}}{\beta^{900}_{Cr_2O_7}}\right)\frac{D_{Cr_2O_7}}{D_{HCrO_4} + 2D_{Cr_2O_7}} \tag{12}$$

According to Eq. (12), any shift in the area ratio must be accompanied by a shift in the relative amounts of bichromate and dichromate.

Under the conditions of high $[Cr^{VI}]$, the equilibrium calculation predicts that the majority species is $Cr_2O_7^{-2}$ and the concentration of bichromate approaches zero. The area ratio becomes constant, dependant only on the magnitude of the cross-sections. In the limit of high $[Cr^{VI}]_{total}$, Eq. (13) applies:

$$\frac{\text{area 219 cm}^{-1}}{\text{area 900 cm}^{-1}} = \left(\frac{2\beta^{219}_{Cr_2O_7}}{\beta^{900}_{Cr_2O_7}}\right)\frac{D_{Cr_2O_7}}{2D_{Cr_2O_7}} = \frac{\beta^{219}_{Cr_2O_7}}{\beta^{900}_{Cr_2O_7}} \tag{13}$$

4. Discussion

The main point of controversy from past research is the existence of bichromate, $HCrO_4^-$, at low pH and low $[Cr^{VI}]_{total}$. Although published equilibrium constants and UV–VIS spectroscopy results require the existence of $HCrO_4^-$, the evidence is derived mainly from analysis of relatively featureless UV–VIS spectra [7–12]. An analysis of more detailed Raman spectra [22] based on band shape changes in the 800–950 cm^{-1} region support the equilibria of Eqs. (1)–(3). However, Raman spectroscopy has also been used to conclude that $HCrO_4^-$ does not exist [19,20], but the low sensitivity of the instrument necessitated the use of high Cr^{VI} concentrations (~0.2 M). Under these conditions, $HCrO_4^-$ is expected to be a minor species. Fig. 7 is based on the equilibria of Eqs. (1)–(3), and demonstrates that Cr^{VI} speciation depends on both pH and $[Cr^{VI}]_{total}$. For $Cr^{VI} = 0.2$ M and pH = 4, only 13% of the Cr^{VI} is $HCrO_4^-$. For a $[Cr^{VI}]_{total}$ of 2 mM, however, $HCrO_4^-$ is expected to be the major species.

With a sufficiently sensitive spectrometer, many observable changes occur in the Raman spectra of Cr^{VI} with both pH and concentration. Of particular note is the 904 cm^{-1} feature and its shift to lower frequency with decreasing Cr^{VI} concentration (Table 3 and Fig. 4). While this phenomenon has been previously observed [22], no significance was assigned. When combined with a broadening of the feature (FWHM), the band shift indicates the formation of a new Raman feature. We have assigned the new band at 898 cm^{-1} to the bichromate species.

More direct evidence for the existence of $HCrO_4^-$ is the observance of the Raman feature at 219 cm^{-1} which has been previously assigned to the Cr–O–Cr bending vibration [30, 31]. As noted earlier, Fig. 6 shows that the fraction of total Cr^{VI} that exists as dichromate decreases with dilution. If dichromate is the only species present, the ratio of the bridging band to the total Cr^{VI} concentration would be constant and equal to a ratio of cross-sections (Eq. (13)). As Fig. 6 clearly illustrates, the band ratio actually decreases with dilution. This effect is predicted from equilibrium calculations, which require a third solution species in addition to $Cr_2O_7^{-2}$ and CrO_4^{-2}; and Eq. (11), which illustrates the sensitivity of the Raman ratio to a

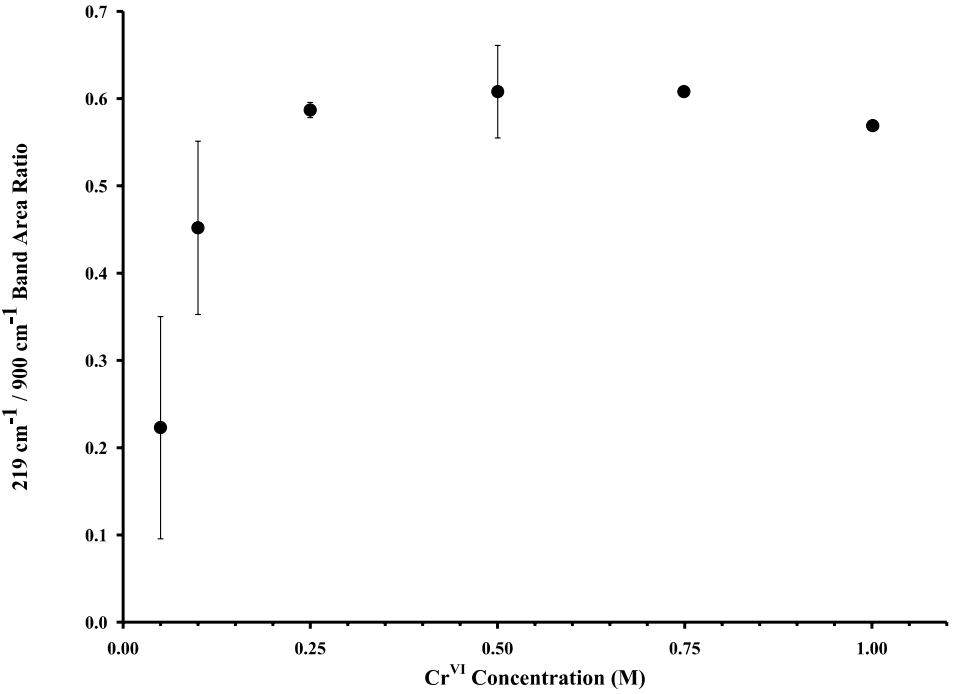

Fig. 6. Plot of the 219–900 cm^{-1} band area ratio versus the concentration of Cr^{VI}. Each solution was adjusted to a pH of 2 and an ionic strength between 1.5 and 2.0 M. Potassium nitrate was used as the ionic strength adjustor.

scatterer in equilibrium with dichromate. These results provide direct evidence for a species other than dichromate in dilute Cr^{VI} solutions of pH < 6, which does not contain a Cr^{VI}–O–Cr^{VI} bond.

According to Eq. (11), the equilibrium calculation data can be directly compared to the Raman ratio data. Fig. 8 shows the calculated $[Cr_2O_7^{-2}]/[Cr^{VI}]_{total}$ ratio superimposed on a plot of the experimental 219 cm^{-1}/900 cm^{-1} area ratio. Note that the ratio does become constant at high $[Cr^{VI}]$, but decreases with dilution. Also of note are the results for nonconstant ionic strength, which show a depressed fraction of Cr^{VI} as dichromate. Literature values of the dimerization constant of bichromate to dichromate show a distinct dependence on the ionic strength. The reported magnitude of K_d ranges from 33 at $\mu < 1$ M to 231 at $\mu = 10$ M [8,16]. Over the range of $[Cr^{VI}]$ studied here, the dimerization constant is dramatically changing resulting in a depression in the 219 cm^{-1}/900 cm^{-1} ratio. When the ionic strength was controlled at 1.5 M, the observed 219 cm^{-1}/900 cm^{-1} intensity ratio closely tracks the $[Cr_2O_7^{-2}]/[Cr^{VI}]_{total}$ ratio calculated from equilibrium constants obtained with $\mu = 1$–1.5 M. This agreement confirms the previous observations which indicate a sensitivity of the dimerization constant to an increased ionic strength while providing evidence for the existence of a monomeric species in equilibrium with dichromate.

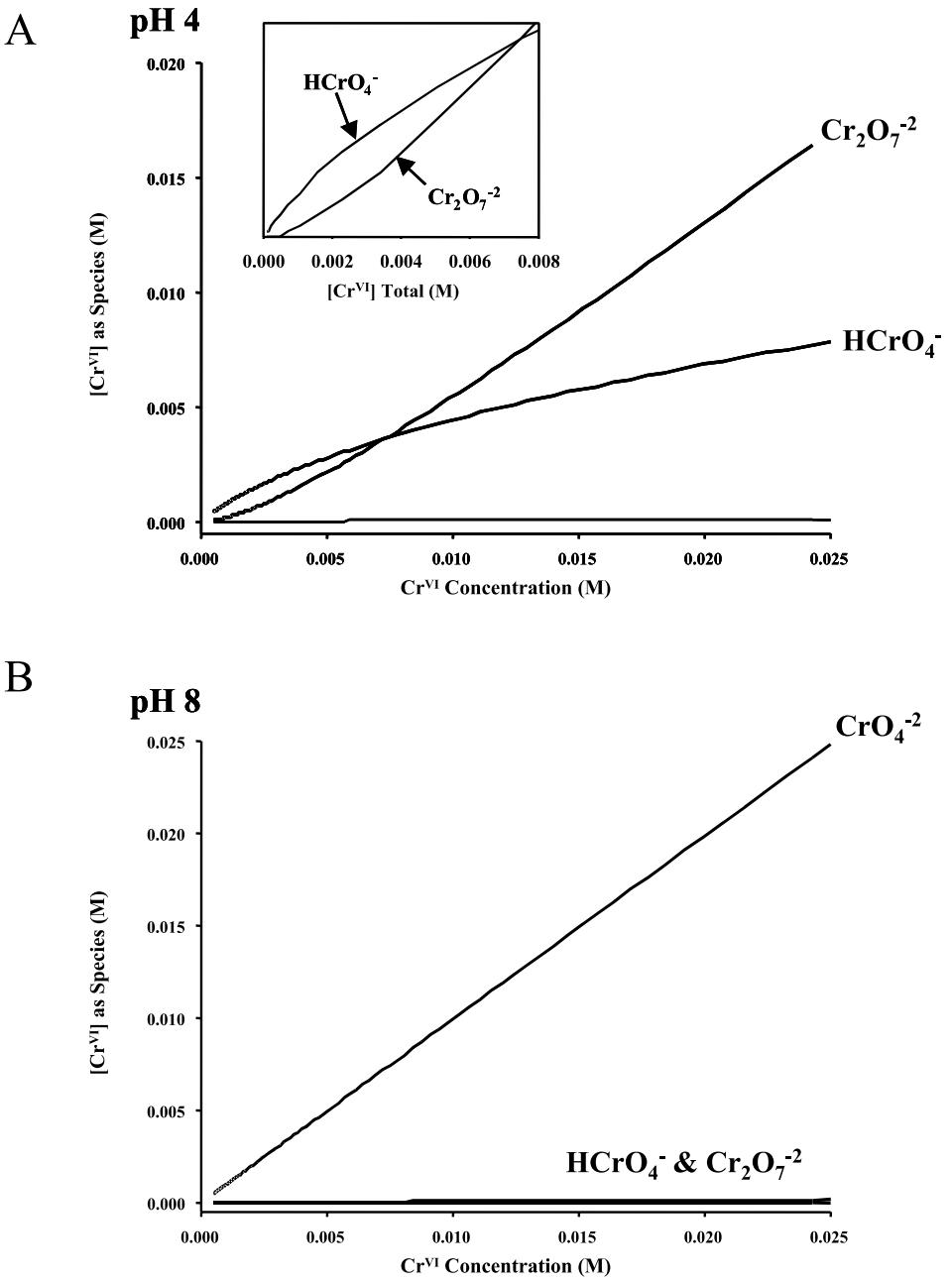

Fig. 7. The calculated distribution of Cr^{VI} species as a function of increasing concentration. A pH of 4 was used to calculate the distribution in plot (A) while a pH of 8 was used for plot (B).

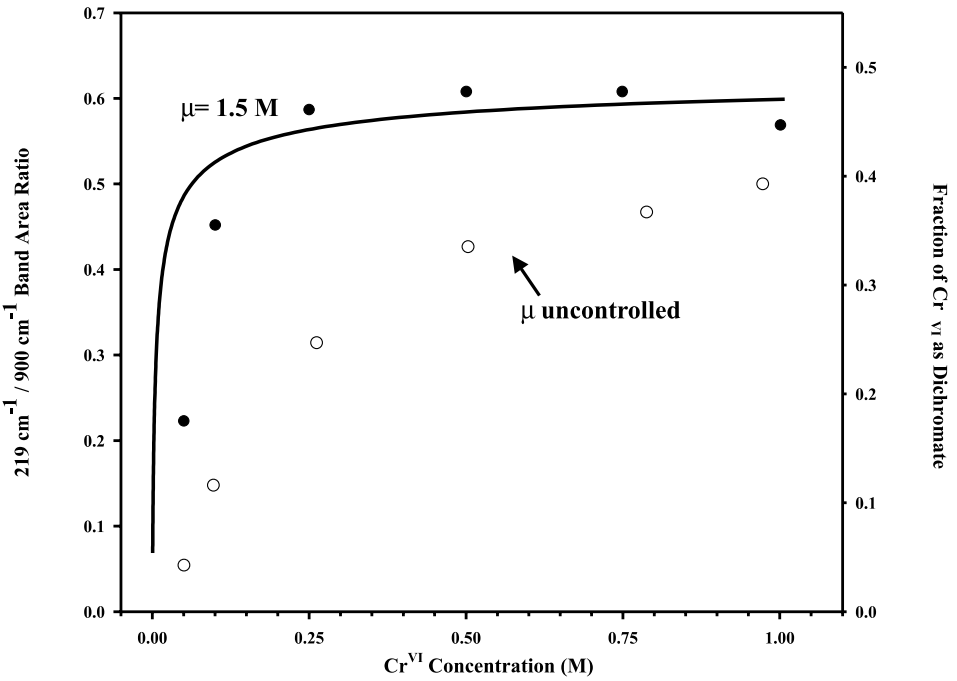

Fig. 8. Plot showing the correlation between the 219 and 900 cm^{-1} band area ratio and the calculated fraction of Cr^{VI} as dichromate. The ratio data for the controlled ionic strength (●) and for no ionic strength (○) are compared to the calculated dichromate fraction (—).

Eqs. (1)–(3) and Table 1 permit determination of the Cr^{VI} species distribution for conditions relevant to corrosion protection. For cathodic regions which are expected to have a pH greater than 7, essentially all Cr^{VI} is CrO_4^{-2}. For conditions common during formation of a chromate conversion coating (e.g. "Alodine"), in which $[Cr^{VI}] \simeq 0.05$ M and pH ~2, about 36% of the Cr^{VI} is $HCrO_4^-$, the remainder is $Cr_2O_7^{-2}$. The $[Cr^{VI}]$ expected in field conditions, such as a damp or damaged chromate coating, is approximately 0.2 mM for Cr^{VI} released from a conversion coating, or ~4.5 mM for saturated $SrCrO_4$ [6]. For these low concentrations and a pH range of 2–6, $HCrO_4^-$ is the dominant Cr^{VI} species, comprising 98% of total Cr^{VI} when $[Cr^{VI}] = 0.2$ mM and 74% when $[Cr^{VI}] = 4.5$ mM. When mechanisms are proposed for corrosion protection by Cr^{VI}, the species distribution of Cr^{VI} may be quite important. For the low $[Cr^{VI}]$ expected during Cr^{VI} protection in mildly acidic conditions $HCrO_4^-$ is the dominant Cr^{VI} species.

5. Conclusions

1. The speciation of Cr^{VI} oxides has been shown to be greatly dependent on both pH and concentration with the monomeric species, $HCrO_4^-$ and CrO_4^{-2}, being the pre-

dominant species under solution conditions most likely encountered in corrosion systems, i.e. at low [Cr^{VI}] and low or high pH.
2. Changes in the Raman spectra of acidic Cr^{VI} solutions upon dilution led to the assignment of a new band at 898 cm^{-1} to a vibration of the bichromate solution species.
3. Direct Raman spectroscopic data clearly illustrates the existence of a monomeric Cr^{VI} species ($HCrO_4^-$) in an environment applicable to corrosion studies which was previously thought to contain only dichromate ($Cr_2O_7^{-2}$).
4. Ionic strength favors the formation of dichromate and justifies the previously published measurements of increasing dimerization constants with increasing ionic strength.
5. In the pH range 2–6 often encountered during corrosion of aluminum alloys, the dominant form of Cr^{VI} at the low concentrations expected in field applications is $HCrO_4^-$ rather than $Cr_2O_7^{-2}$.

Acknowledgements

This work was supported by the Air Force Office of Scientific research, contract # F49620-96-1-0479. The authors wish to thank Gerald Frankel for useful suggestions during this research.

References

[1] L. Xia, R.L. McCreery, J. Electrochem. Soc. 145 (9) (1998) 3083.
[2] J. Zhao, G. Frankel, R.L. McCreery, J. Electrochem. Soc. 145 (7) (1998) 2258.
[3] J.D. Ramsey, R.L. McCreery, J. Electrochem. Soc. 146 (11) (1999) 4076.
[4] E. McCafferty, J. Electrochem. Soc. 137 (12) (1990) 3731.
[5] M. Kendig, R. Addison, S. Jeanjaquet, J. Electrochem. Soc. 146 (12) (1999) 4419.
[6] L. Xia, E. Akiyama, G. Frankel, R. McCreery, J. Electrochem. Soc. 147 (7) (2000) 2556.
[7] J.Y. Tong, E.L. King, J. Am. Chem. Soc. 75 (1953) 6180.
[8] W.G. Davies, J.E. Prue, J. Faraday Soc. 51 (1955) 1045.
[9] N. Bailey, A. Carrington, K.A.K. Lott, M.C.R. Symons, J. Chem. Soc. (1960) 290.
[10] G.P. Haight Jr., D.C. Richardson, N.H. Coburn, Inorg. Chem. 3 (1964) 1777.
[11] M.A. Olazabal, G. Borge, R. Castano, N. Etxebarria, J.M. Madariaga, J. Sol. Chem. 22 (9) (1993) 825.
[12] J.J. Cruywagon, J.B.B. Heyns, E.A. Rohwer, Polyhedron 17 (10) (1998) 1741.
[13] J.D. Neuss, W. Rieman III, J. Am. Chem. Soc. 56 (1934) 2238.
[14] Y. Sasaki, Acta Chem. Scand. 16 (1962) 719.
[15] J.G. Mason, A.D. Kowalak, Inorg. Chem. 3 (1964) 1248.
[16] D.V.S. Jain, C.M. Jain, J. Chem. Soc. A (1967) 1541.
[17] N.E. Brasch, D.A. Buckingham, A.B. Evans, C.R. Clark, J. Am. Chem. Soc. 118 (1996) 7969.
[18] N.E. Brasch, D.A. Buckingham, C.R. Clark, A.E. Rowan, Aust. J. Chem. 49 (1996) 697.
[19] G. Michel, R. Machiroux, J. Raman Spectrosc. 14 (1983) 22.
[20] G. Michel, R. Cahay, J. Raman Spectrosc. 17 (1986) 79.
[21] V.G. Poulopoulou, E. Vrachnou, S. Koinis, D. Katakis, Polyhedron 16 (3) (1997) 521.
[22] J.B.B. Heyns, J.J. Cruywagen, K.T. Carron, J. Raman Spectrosc. 30 (1999) 335.

[23] S. Veritt, L.S. Levy, Nature 250 (1974) 493.
[24] P. Sanz, J.L. Moline, D. Sole, J. Corbella, J. Occup. Med. 31 (12) (1989) 1013.
[25] S.A. Katz, H. Salem, The Biological and Environmental Chemistry of Chromium, VCH, New York, 1994, p. 6.
[26] B.M. Weckhuysen, I.E. Wachs, R.A. Schoonheydt, Chem. Rev. 96 (1996) 3327.
[27] R.K. Tandon, P.T. Crisp, J. Ellis, R.S. Baker, Talanta 31 (3) (1984) 227.
[28] T. Shen-Yang, L. Ke-An, Talanta 33 (9) (1986) 775.
[29] M. Kendig, J. Ramsey, R. McCreery, L. Xia, Speciation of oxo-Cr(VI) anions and the corrosion inhibition of aluminum alloys, Proceedings of the Sato Symposium, Electrochemical Society, 1999.
[30] H. Stammreich, D. Bassi, D. Sala, H. Siebert, Spectrochim. Acta 13 (1958) 192.
[31] J.E.D. Davies, D.A. Long, J. Chem. Soc. A (1971) 1275.
[32] K. Nakamoto, Infrared and Raman Spectra of Inorganic and Coordination Compounds, Part A, Wiley, New York, 1997, pp. 199–200.
[33] N. Weinstock, H. Schulze, A. Müeller, J. Chem. Phys. 59 (9) (1973) 5063.
[34] R.L. McCreery, in: J.V. Sweedler, K.L. Ratzlaff, M.B. Denton (Eds.), Charge-Transfer Devices in Spectroscopy, VCH, New York, 1994, pp. 227–279.